

Gapped spin-liquid phase in the J_1 - J_2 Heisenberg model by a bosonic resonating valence-bond ansatz

Tao Li,^{1,2} Federico Becca,² Wenjun Hu,² and Sandro Sorella²¹*Department of Physics, Renmin University of China, Beijing 100872, People's Republic of China*²*SISSA–International School for Advanced Studies and CNR-IOM Istituto Officina dei Materiali, Democritos Center, Via Bonomea 265, 34136 Trieste, Italy*

(Received 21 May 2012; published 7 August 2012)

We study the ground-state phase diagram of the spin-1/2 J_1 - J_2 Heisenberg model on the square lattice with an accurate bosonic resonating-valence-bond (RVB) wave function. In contrast to the RVB ansatz based on Schwinger fermions, the representation based on Schwinger bosons, supplemented by a variational Monte Carlo technique enforcing the exact projection onto the physical subspace, is able to describe a fully gapped spin liquid in the strongly frustrated regime. In particular, a fully symmetric Z_2 spin liquid is stable between two antiferromagnetic phases; a continuous transition at $J_2 = 0.4J_1$, when the Marshall sign rule begins to be essentially violated, and a first-order transition around $J_2 = 0.6J_1$ are present. Most importantly, the triplet gap is found to have a nonmonotonic behavior, reaching a maximum around $J_2 = 0.51J_1$, when the lowest spinon excitation moves from the Γ to the M point, i.e., $k = (\pi, 0)$.

DOI: [10.1103/PhysRevB.86.075111](https://doi.org/10.1103/PhysRevB.86.075111)

PACS number(s): 75.10.Kt, 75.10.Jm

I. INTRODUCTION

The search for quantum spin liquids in frustrated quantum antiferromagnets has a long history.¹ In recent years, thanks to the advance of numerical techniques, several candidates for spin liquids have emerged in two-dimensional systems. These include the Hubbard model on the honeycomb lattice,² the spin-1/2 Heisenberg model on the kagome lattice,³ and more recently the spin-1/2 J_1 - J_2 Heisenberg model on the square lattice.⁴ In all these cases, a small but finite spin gap has been found and, according to generalizations of the Lieb-Schultz-Mattis theorem for higher dimensionalities,⁵ a topological degeneracy is expected. In spite of these results, descriptions based upon fermionic resonating-valence-bond (RVB) theory predict more often the existence of gapless spin-liquid states. For example, for the J_1 - J_2 model on the square lattice,⁶ the Heisenberg model on the triangular⁷ or the kagome lattice,⁸ and, more recently, also for the unfrustrated honeycomb lattice,⁹ the fermionic RVB theory always predicts a gapless spin-liquid phase with a Dirac-type spinon dispersion as the best variational state.

The J_1 - J_2 model represents the simplest model to study the effect of frustration in a (low-dimensional) magnetic system; for this reason it has been investigated by many different approaches in the last 20 years.^{10–17} At the classical level, the system is magnetically ordered for $J_2 < 0.5J_1$ with the standard antiferromagnetic pattern at $q = (\pi, \pi)$. For $J_2 > 0.5J_1$, the ordering wave vector is moved to $q = (\pi, 0)$ or $(0, \pi)$; these two ordered phases are separated by a first-order transition. Within the linear spin-wave approach, which goes beyond the classical theory, quantum fluctuations destroy the magnetic order in the intermediate region of $0.4J_1 \lesssim J_2 \lesssim 0.6J_1$, hence leading to a magnetically disordered state.¹⁸ However, the nature of this disordered phase is still elusive and several proposals have been made. These include valence-bond solids with broken spatial symmetries^{11,14,19,20} or gapless spin-liquid states.⁶ The latter proposal is especially attractive, since it provides a simple and very accurate fermionic RVB wave

function for $0.4J_1 \lesssim J_2 \lesssim 0.55J_1$. This state has a Dirac-type spinon dispersion and Z_2 gauge structure and becomes stable for $J_2 \gtrsim 0.4J_1$.

More recently, density-matrix renormalization-group (DMRG) calculations provided some evidence for a fully gapped spin liquid in the intermediate region of $0.4J_1 \lesssim J_2 \lesssim 0.62J_1$.⁴ Within this numerical approach, the spin gap increases linearly from $J_2 \simeq 0.4J_1$, reaches a maximum around $J_2 \simeq 0.59J_1$, and then rapidly decreases. For $J_2 \gtrsim 0.62J_1$, a collinear magnetic order occurs. The spin-liquid phase determined by these DMRG calculations is thus inconsistent with the fermionic RVB theory, due to the presence of a finite spin gap.

In this paper, we investigate the spin-liquid phase of the J_1 - J_2 model with a bosonic RVB wave function.²¹ This is motivated by the following concerns. First, while the fermionic RVB state is found to be unable to open a spin gap for this system, a bosonic spin-liquid state is by definition gapped, because otherwise the (bosonic) spinon would condense and the system would develop magnetic order. Second, since the spin-liquid phase is found to exist in a quite small region between two magnetically ordered phases (for which a bosonic description is quite accurate), it is natural to expect that the intermediate spin-liquid phase inherits some bosonic characteristic.

The bosonic RVB state has been adopted in many previous studies^{22,23} and is found to describe quite well both the magnetic ordered state and the disordered state for unfrustrated systems.^{24,25} For frustrated magnetic systems, the use of the bosonic RVB wave function is very limited, since the loop gas algorithm for the bosonic RVB state encounters serious sign problems; moreover, the computation of the wave function amplitude in the orthogonal Ising basis involves permanents of matrices,²⁶ implying a computational cost that grows exponentially with the size of the system. Only very recently has this approach been implemented on small clusters for the kagome lattice.²⁷

Here, the bosonic RVB state is obtained after projecting the ground state of the mean-field Schwinger-boson Hamiltonian²⁸ into the physical subspace with one spin per site. After this projection, the wave function turns out to be equivalent to the standard Liang-Doucot-Anderson RVB ansatz,²¹ defined only in terms of a bosonic pairing function (that connects opposite sublattices). To enforce the physical symmetry of the model in the RVB state, we have made a full symmetry classification of the Schwinger-boson mean-field ansatz on the square lattice with the projective symmetry group (PSG) technique.²⁹⁻³¹ Then, we have performed variational Monte Carlo simulations in order to optimize such a bosonic RVB state, by using both the permanent Monte Carlo algorithm and the loop gas algorithm.

We find that the bosonic RVB wave function gives a rather good variational description of the system. In addition, we find that the phase diagram predicted by the DMRG calculations can be well reproduced. More specifically, the system is found to enter a fully gapped spin-liquid state around $J_2 = 0.4J_1$ through a continuous transition, when the Marshall sign rule in the ground state begins to be essentially violated. A level crossing of the spinon excitation is observed around $J_2 = 0.51J_1$, when the gap minimum of the spinon excitation branch is moved from the Γ to the M [i.e., $k = (\pi, 0)$] point and a kink appears in the spin gap as a function of J_2 .

Finally, by PSG symmetry considerations, it can be shown that the spin gap is always finite at the M point in the spin-liquid region [while it can vanish at (π, π) , at the transition to the antiferromagnetic phase for small J_2]. This fact implies that the magnetic structure factor is always finite at the M point, ruling out a continuous transition to the collinear phase at large J_2 .

The paper is organized as follows: in Sec. II, we describe the model and the method; in Sec. III, we present our numerical results; finally, in Sec. IV, we draw our conclusions.

II. THE MODEL AND METHODS

In this paper, we consider the following model:

$$H = J_1 \sum_{\langle i, j \rangle} \vec{S}_i \cdot \vec{S}_j + J_2 \sum_{\langle\langle i, j \rangle\rangle} \vec{S}_i \cdot \vec{S}_j, \quad (1)$$

where $\langle i, j \rangle$ and $\langle\langle i, j \rangle\rangle$ indicate nearest-neighbor and next-nearest-neighbor sites on the square lattice, respectively; \vec{S}_i denotes the spin operator at site i .

In the Schwinger-boson representation,²⁸ the spin operator is written as $\vec{S}_i = \frac{1}{2} \sum_{\alpha, \beta} b_{i\alpha}^\dagger \vec{\sigma}_{\alpha, \beta} b_{i\beta}$, where $b_{i\alpha}$ is a boson operator and $\vec{\sigma}$ is the Pauli matrix. Bosons should satisfy the no-double-occupancy constraint $\sum_{\alpha} b_{i\alpha}^\dagger b_{i\alpha} = 1$, in order to be a faithful representation of the spin-1/2 operator. Within this representation, the Heisenberg superexchange coupling can be written as (apart from additive constants) $\vec{S}_i \cdot \vec{S}_j = -\frac{1}{2} \hat{A}_{i,j}^\dagger \hat{A}_{i,j} = \frac{1}{2} \hat{B}_{i,j}^\dagger \hat{B}_{i,j}$, where $\hat{A}_{i,j} = b_{i\uparrow} b_{j\downarrow} - b_{i\downarrow} b_{j\uparrow}$ and $\hat{B}_{i,j} = b_{i\uparrow}^\dagger b_{j\uparrow} + b_{i\downarrow}^\dagger b_{j\downarrow}$.²⁸

In the mean-field treatment, we replace $\hat{A}_{i,j}$ and $\hat{B}_{i,j}$ with their mean-field expectation values $A_{i,j}$ and $B_{i,j}$, so

we have

$$\begin{aligned} H_{\text{MF}} = & -\frac{1}{2} \sum_{i,j} (\Delta_{i,j} \hat{A}_{i,j}^\dagger + \text{H.c.}) \\ & + \frac{1}{2} \sum_{i,j} (F_{i,j} \hat{B}_{i,j}^\dagger + \text{H.c.}) \\ & + \lambda \sum_i \left(\sum_{\alpha} b_{i\alpha}^\dagger b_{i\alpha} - 1 \right), \end{aligned} \quad (2)$$

where $\Delta_{i,j} = J_{i,j} A_{i,j}$, $F_{i,j} = J_{i,j} B_{i,j}$, and the chemical potential λ is introduced to fulfill, on average, the single-occupancy constraint. The mean-field ground state has the general form of

$$|\text{MF}\rangle \propto \exp \left\{ \sum_{i,j} a(R_i, R_j) (b_{i\uparrow}^\dagger b_{j\downarrow}^\dagger - b_{i\downarrow}^\dagger b_{j\uparrow}^\dagger) \right\} |0\rangle. \quad (3)$$

Then, a suitable RVB wave function in the *physical* Hilbert space with one boson per site may be obtained by projecting the mean-field state, namely,

$$|\text{RVB}\rangle = P_G |\text{MF}\rangle, \quad (4)$$

where P_G is a Gutzwiller projector that enforces the constraint of one boson per site. The equivalence of the RVB state with the standard Liang-Doucot-Anderson state²¹ is clear after projection onto the physical subspace.

The form of the RVB amplitude $a(R_i, R_j)$ is determined by the parameters $\Delta_{i,j}$, $F_{i,j}$, and λ . At the mean-field level, $\Delta_{i,j}$ and $F_{i,j}$ are nonzero only on those bonds with $J_{i,j} \neq 0$. However, from the variational point of view, we can take $\{\Delta_{i,j}, F_{i,j}, \lambda\}$ as a set of free parameters to construct the RVB state. In such a case, we can also introduce $\Delta_{i,j}$ and $F_{i,j}$ on longer bonds, for which $J_{i,j} = 0$.

In order to describe a spin-liquid state with the *full* symmetry of the model, the mean-field parameters $\{\Delta_{i,j}, F_{i,j}, \lambda\}$ must satisfy certain symmetry conditions. Since there exists a U(1) gauge degree of freedom in the Schwinger-boson representation of the spin operator (i.e., $b_{i\alpha} \rightarrow b_{i\alpha} e^{i\phi_i}$ leaves \vec{S}_i unchanged), the symmetry requirement on the mean-field Hamiltonian is actually the U(1) gauge projective extension of the physical symmetry of the model. Such symmetry conditions on the mean-field ansatz can be readily worked out by the so-called PSG technique developed by Wen²⁹ for the fermionic representation. The bosonic version of the PSG is the U(1) subset of the fermionic PSG.^{30,31} Here, we will just point out some basic structures that are relevant to our study.

In the Schwinger-boson formalism, the mean-field parameters $\Delta_{i,j}$ and $F_{i,j}$ describe antiferromagnetic and ferromagnetic local correlations, respectively (see Appendix A for the possible phases implied by this ansatz). Here, we assume a nonzero $\Delta_{i,j}$ between nearest-neighbor sites. Then, we find that a nonzero $\Delta_{i,j}$ between next-nearest-neighbor sites is compatible only with the so-called type-B translational property of the mean-field Hamiltonian,^{29,30} which implies a unit cell with two sites. We find that such a state is much higher in energy than any state in the so-called type-A class, characterized by a manifestly translationally invariant mean-field ansatz. Therefore, in the following we restrict our

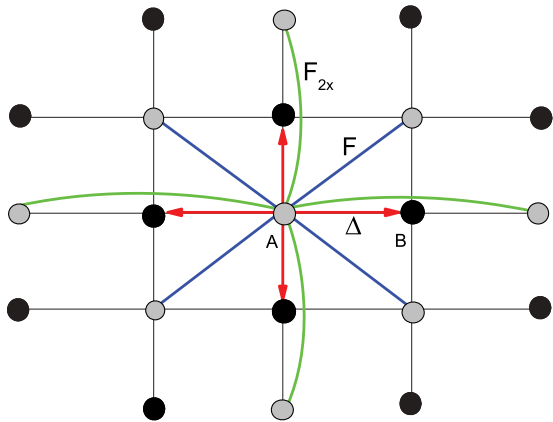


FIG. 1. (Color online) An illustration of the mean-field parameters starting from a site in the sublattice A. Gray and dark dots denote sites in sublattices A and B. Here, only bonds up to the third neighbors are reported, since longer-range parameters are found to be negligibly small after optimization. The pairing term is always directed from sublattice A to sublattice B.

analysis only to translationally invariant states. Within the type-A states, we find the following general rules for the mean-field ansatz for a symmetric spin-liquid state. First, for sites belonging to different sublattices, only a *real* $\Delta_{i,j}$ is allowed. Second, for sites in the same sublattice, only a *real* $F_{i,j}$ is allowed. Considering the site i as belonging to the A sublattice,³² the allowed mean-field parameters up to the fourth neighbor are given by

$$F_{i,i+\bar{\delta}_1} = 0, \quad \Delta_{i,i+\bar{\delta}_1} = \Delta, \quad (5)$$

$$F_{i,i+\bar{\delta}_2} = F, \quad \Delta_{i,i+\bar{\delta}_2} = 0, \quad (6)$$

$$F_{i,i+\bar{\delta}_3} = F_{2x}, \quad \Delta_{i,i+\bar{\delta}_3} = 0, \quad (7)$$

$$F_{i,i+\bar{\delta}_4} = 0, \quad \Delta_{i,i+\bar{\delta}_4} = \Delta_{2xy}, \quad (8)$$

where $\bar{\delta}_\mu$ (with $\mu = 1, \dots, 4$) denotes the vectors connecting the site i to its neighbors, up to the fourth distance. Here, $\{\lambda, F, \Delta, F_{2x}, \Delta_{2xy}\}$ are a set of real parameters. An illustration of the ansatz used in this study is shown in Fig. 1. For the sites i belonging to the B sublattice, the signs of Δ and Δ_{2xy} should be reversed (since $\Delta_{i,j}$ is odd on interchanging i and j).

At the mean-field level, both F_{2x} and Δ_{2xy} are zero, and the Hamiltonian is given by

$$H_{\text{MF}} = \sum_{k \in \text{MBZ}} \psi_k^\dagger \begin{pmatrix} \epsilon_k & 0 & 0 & \Delta_k \\ 0 & \epsilon_k & -\Delta_k & 0 \\ 0 & -\Delta_k & \epsilon_k & 0 \\ \Delta_k & 0 & 0 & \epsilon_k \end{pmatrix} \psi_k, \quad (9)$$

in which MBZ indicates the reduced (magnetic) Brillouin zone, $\psi_k^\dagger = (b_{Ak\uparrow}^\dagger, b_{Bk\uparrow}^\dagger, b_{A-k\downarrow}, b_{B-k\downarrow})$, $\epsilon_k = \lambda + 2Fg(k)$, and $\Delta_k = 2\Delta\gamma(k)$. Here $g(k) = \cos(k_x)\cos(k_y)$ and $\gamma(k) = [\cos(k_x) + \cos(k_y)]/2$. The mean-field spectrum is given by $E_k = \sqrt{\epsilon_k^2 - \Delta_k^2}$ and the minimal spinon gap is given by

$$E_{\text{min}} = \begin{cases} \sqrt{(\lambda + 2F)^2 - (2\Delta)^2}, & 2\lambda F < \Delta^2, \\ \lambda - 2F, & 2\lambda F > \Delta^2. \end{cases}$$

For the first case, the gap minimum is located at the Γ point, while for the second case the gap minimum is at the M point.

Finally, the RVB amplitudes derived from the mean-field ground state are given by

$$a(R_i - R_j) = \frac{1}{N} \sum_{k \in \text{MBZ}} \frac{\Delta_k}{\epsilon_k + E_k} e^{ik \cdot (R_i - R_j)}, \quad (10)$$

where N is the number of sites, $i \in A$, and $j \in B$. The RVB amplitudes between sites in the same sublattice are identically zero. We would like to mention that, within the standard formulation based upon Monte Carlo sampling,²¹⁻²³ only positive pairing functions $a(R_i - R_j)$ have been considered so far. In our formulation this restriction applies only for standard antiferromagnetic phases, while negative amplitudes are found in the much more interesting spin-liquid phase.

III. RESULTS

The mean-field Hamiltonian (9) has been studied by Mila and collaborators,³³ showing that no spin-liquid phases are stabilized and a direct transition between two ordered phases is present, with a phase diagram that is very similar to that in the classical limit. In order to go beyond this approximation, we now move to the *projected* RVB state of Eq. (4), to assess the possibility that quantum fluctuations may induce a finite spin gap and, therefore, a stable spin liquid. We thus determine the parameters in the bosonic RVB state by optimizing the energy of the original J_1 - J_2 model rather than by solving the self-consistent equations. Then, the spinon gap can be estimated by inserting back the optimized parameters into the mean-field dispersion relation E_k . Note that the RVB wave function does not depend on the overall energy scale of the system. As a result, the spinon gap can be determined only up to a normalization constant. Here we will use the chemical potential λ as the unit of energy. To have an estimate of the absolute scale of the spinon gap, we determine the pairing potential Δ from the equation

$$\Delta = J_1 \langle \hat{A}_{i,i+x} \rangle = \frac{J_1}{N} \sum_{k \in \text{MBZ}} \frac{\Delta_k \gamma(k)}{E_k} \quad (11)$$

by inserting on the right-hand side the optimized values of Δ/λ and F/λ , which are $(\Delta/\lambda)_{\text{opt}}$ and $(F/\lambda)_{\text{opt}}$. Then λ can be determined by requiring that $\Delta/\lambda = (\Delta/\lambda)_{\text{opt}}$.

The computation of the bosonic RVB wave function is very expensive in the Ising basis, since it requires the calculation of permanents, for which no polynomial algorithm exists.²⁶ However, on small clusters the calculation is still affordable. In this work, we have used a 6×6 cluster to perform the optimization of the parameters in the RVB wave function.³⁴ It is important to note the key difference between the mean-field theory and the projected RVB wave function. In the mean-field theory, the chemical potential λ is determined by the self-consistent equation for the total boson number. When the spinon gap approaches zero, the number of bosons will diverge. Thus, on any finite lattice, the spinon gap can never be zero and a finite-size gap must exist (see Appendix B for the details on the spinon gap in the mean-field approach). On the contrary, after projection, the constraint of one boson per site is satisfied *exactly* and such a divergence will not appear. Therefore, the

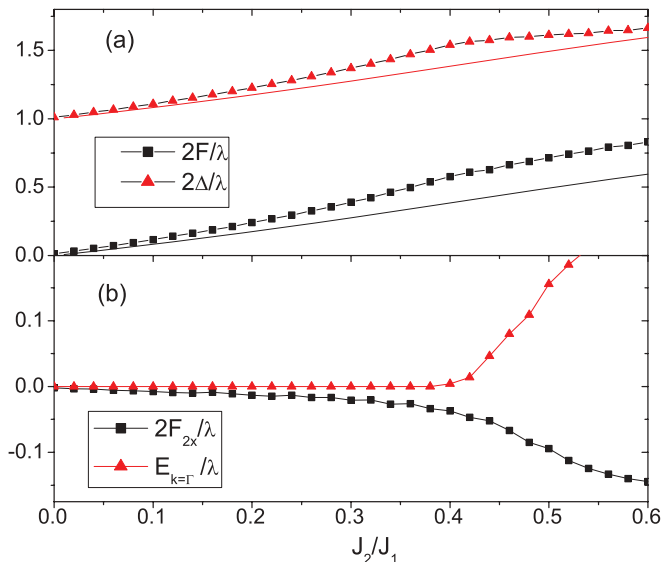


FIG. 2. (Color online) (a) The optimized values for various parameters $2F/\lambda$ and $2\Delta/\lambda$. The lines without symbols denote the solutions of the mean-field self-consistent equations. (b) $2F_{2x}/\lambda$ and the (normalized) spinon gap at the Γ point.

RVB wave function is well behaved even when the spinon gap is zero. This fact implies that a vanishing spinon gap can be realized exactly after optimization of the corresponding projected RVB wave function on a relatively small cluster.

From our numerical optimization, we find that a spin gap cannot be opened if we keep Δ/λ and F/λ only. Moreover, by a direct optimization of the pairing amplitudes $a(R_i - R_j)$, a good accuracy can be achieved only by including a third-neighbor parameter F_{2x}/λ , while the fourth-neighbor parameter Δ_{2xy}/λ is found to always negligibly small. Therefore, in the following, we optimize the wave function with Δ/λ , F/λ , and F_{2x}/λ as variational parameters. In particular, we find that the inclusion of F_{2x}/λ is crucial for the opening of the spin gap. The optimized values of the parameters in the RVB wave function are shown in Fig. 2.

The spinon gap at the Γ and the M points is shown in Fig. 3(a). Around $J_2 = 0.51J_1$, a level crossing in the spinon excitation occurs and the gap minimum changes from Γ to M . By further increasing J_2 , the spinon gap at M decreases and eventually approaches zero around $J_2 = 0.6J_1$. At this point the system becomes unstable with respect to magnetic ordering at $q = (\pi, 0)$. It should be noted that, although the spinon gap at the M point approaches zero continuously for $J_2 = 0.6J_1$, our state cannot be continuously connected to the collinear ordered state, and a first-order transition must exist between the fully symmetric spin liquid and the collinear ordered magnetic phase. This is clearly seen in the static spin structure factor:

$$S(q) = \frac{1}{2} \sum_k \left(\frac{\epsilon_k \epsilon_{q-k} - \Delta_k \Delta_{q-k}}{E_k E_{q-k}} - 1 \right). \quad (12)$$

Since $\Delta_{k=(\pi,0)} = 0$ by symmetry (see Appendix C), the singularity in the coherence factor for $E_{k=(\pi,0)} \rightarrow 0$ is removed and the spin structure factor at $q = (\pi, 0)$ is always finite. Thus, the state cannot be connected to the collinear ordered

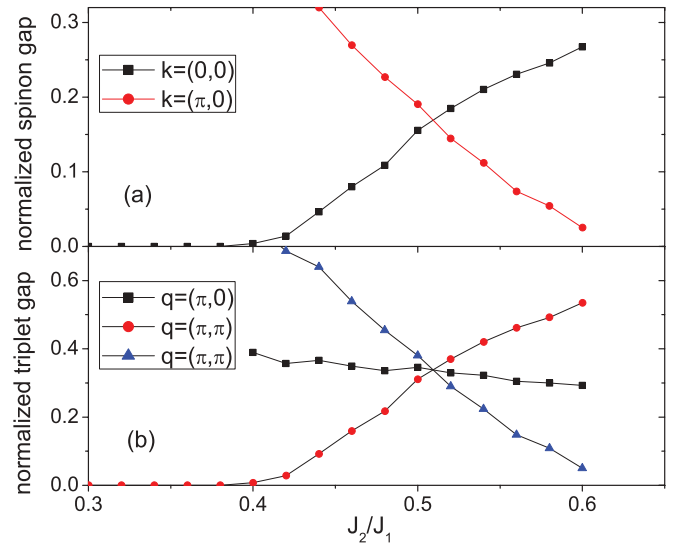


FIG. 3. (Color online) (a) The normalized spinon gap at the Γ and M points in the spin-liquid regime. (b) Normalized triplet gap at $q = (\pi, \pi)$ and $q = (\pi, 0)$ (b).

phase, in which $S(\pi, 0)$ diverges. Therefore, we conclude that a first-order transition must exist between the spin liquid and the collinear ordered phase.

Given the results for the spinon spectrum of Fig. 3(a), it is possible to make some prediction on the behavior of the triplet gap as a function of J_2 . Indeed, to construct a triplet excitation at $q = (\pi, \pi)$, we can use two spinons both from either the Γ point or the M point.³⁵ On the contrary, for a triplet excitation with momentum $q = (\pi, 0)$, we should use one spinon from the Γ point and another spinon from the M point. Therefore, the lowest triplet excitation is always realized at $q = (\pi, \pi)$ and the energy of triplet excitation at $q = (\pi, 0)$ is always finite; see Fig. 3(b). This is consistent with the result of the static spin structure factor mentioned above and points to the fact that our spin-liquid state cannot be continuously connected to the collinear ordered phase. We note that the peculiar behavior of the triplet excitations found in this work represents a surprising consequence of fractionalized spinon excitations in the spin-liquid phase.

We would like to mention that our results for the spin gap are quite similar to those from the DMRG calculations.⁴ Indeed, within both approaches, the spin gap is found to open around $J_2 = 0.4J_1$ and close around $J_2 = 0.62J_1$. In addition, a sharp maximum is present, although its position in the bosonic RVB approach is found to correspond to a lower value of J_2 with respect to the DMRG study. Moreover, taking the value of λ estimated from Eq. (11), which is $\lambda \approx 1.02J_1$ at $J_2 = 0.5J_1$, we have that the maximal spin gap is quite consistent with the DMRG prediction.

In this work, the sharp maximum in the spin gap is interpreted as the result of a level crossing in the minimum of the spinon spectrum (from the Γ to the M point). In such a picture the lowest triplet excitation within the symmetric spin-liquid phase is always at $q = (\pi, \pi)$. However, other possibilities for this structure may exist, among which a nematic spin-liquid phase, which breaks the reflection symmetry $x \rightarrow y$ but with all other physical symmetries intact, is especially interesting.³⁶

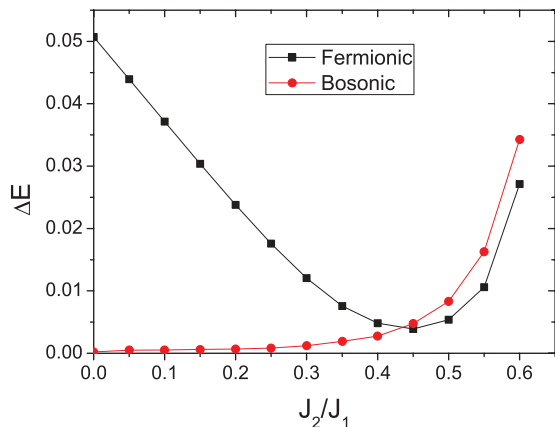


FIG. 4. (Color online) Accuracy of the ground-state energy calculated from the best fermionic of Ref. 6 and bosonic RVB variational wave functions on a 6×6 lattice.

Since the DMRG calculations have been done on rectangular clusters, the nematic liquid phase can be connected to the symmetric state continuously on finite lattices.

To further check the accuracy of the bosonic RVB wave function, we computed the relative error in the ground-state energy, namely, $\Delta E = |E_0 - E_{\text{var}}|/|E_0|$, where E_0 is the exact ground-state energy and E_{var} is the variational energy of the RVB state. In Fig. 4, we report the accuracy of the bosonic RVB wave function on the 6×6 cluster, in comparison with the best fermionic RVB wave function.⁶ For small J_2 , the bosonic RVB wave function is much more accurate than the fermionic RVB wave function, which cannot describe magnetically ordered states. In this region, our results for the bosonic wave function agree with previous calculations reported in Ref. 37, obtained with a different algorithm²² or a different parametrization.²³ For $J_2 \gtrsim 0.45J_1$, the fermionic wave function becomes more accurate. However, the errors in both wave functions are similar and both increase with the same trend on increasing J_2 up to $J_2 = 0.6J_1$.

As pointed out in Ref. 6, the sign structure of the ground state is crucial for the origin of the spin-liquid phase. For $J_2 = 0$, the ground-state wave function satisfies the Marshall sign rule.³⁸ However, the Marshall sign rule is essentially violated only for $J_2 \gtrsim 0.4J_1$ and, in the fermionic RVB approach, a Z_2 spin-liquid phase emerges just at the same point.⁶ A similar scenario also appears in the bosonic representation. In this case, when the RVB amplitudes from sublattice A to sublattice B are positive, then the wave function satisfies the Marshall sign rule; otherwise (if some amplitudes are negative) the Marshall sign rule is violated. In Fig. 5, we plot all the independent RVB amplitudes $a(R_i, R_j)$ on a 6×6 lattice of the optimized wave function (with the amplitude between the nearest-neighbor sites equal to 1). For $J_2 < 0.4J_1$, all amplitudes are positive and thus the wave function has the Marshall sign. For $J_2 > 0.4J_1$, the amplitude on bond (1,2) becomes negative and the Marshall sign rule is violated. It is just at this point that the spin gap opens. Thus, the origin of the spin gap and the existence of the spin-liquid phase can be understood as a result of violation of the Marshall sign rule. Such an understanding is consistent with several previous studies,³⁹ in which the topological degeneracy, which

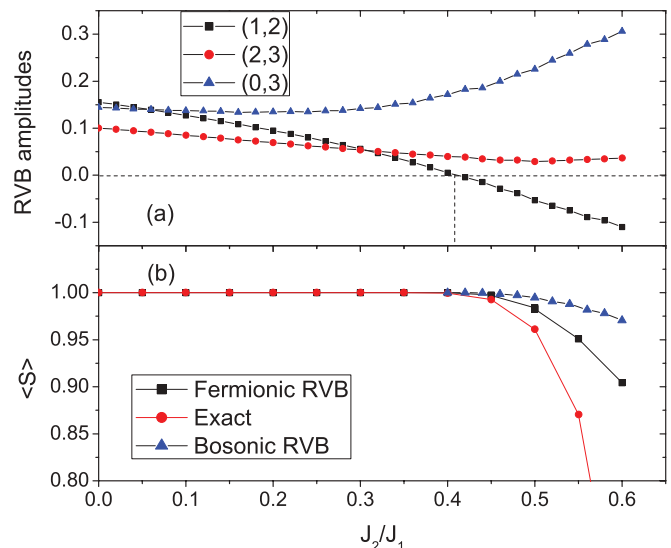


FIG. 5. (Color online) (a) The normalized RVB amplitudes $a(R_i, R_j)$ at different distances on a 6×6 lattice as functions of J_2/J_1 . The nearest-neighbor (1,0) amplitude has been taken equal to 1. (b) The average Marshall sign of Eq. (13) calculated from the bosonic and fermionic RVB wave functions and the exact ground state on a 6×6 lattice as a function of J_2/J_1 .

is a hallmark of gapped spin liquids, is argued to be absent in systems satisfying the Marshall sign rule.

Finally, we report in Fig. 5 the average Marshall signs in the bosonic and fermionic RVB wave functions:

$$\langle S \rangle = \sum_x |\langle x | \text{RVB} \rangle|^2 \text{sgn}\{\langle x | \text{RVB} \rangle (-1)^{N_\uparrow(x)}\}, \quad (13)$$

where $|\text{RVB}\rangle$ denotes the RVB variational state (either bosonic or fermionic) and the sum is over the orthogonal Ising basis $|x\rangle$; for comparison, we also report the results for the exact ground state, where $|\text{RVB}\rangle$ is replaced by $|\Psi_0\rangle$. The fermionic RVB wave function is better in the sense of sign structure, and this is consistent with the fact that the fermionic wave function has a lower energy for large J_2 . However, it is clearly seen that both the bosonic and the fermionic RVB wave functions underestimate seriously the frustration of the sign in the spin-liquid regime.

IV. CONCLUSIONS

In conclusion, we find that the bosonic RVB wave function generates a ground-state phase diagram of the J_1 - J_2 model on the square lattice that is qualitatively consistent with DMRG results. A gapped spin-liquid phase is found for $0.4J_1 < J_2 < 0.6J_1$. The spin-liquid phase is connected to the staggered magnetic ordered state through a continuous transition but cannot be connected continuously to the collinear magnetic ordered state, and a first-order transition between the two must exist. The spin gap is found to have a maximum around $J_2 = 0.51J_1$, as a result of the level crossing between the spinons at Γ and M points. This fact implies that the lowest triplet excitation is found to be always at $q = (\pi, \pi)$ in the spin-liquid phase. We also found that the spin gap opens at the same point where the system violates the Marshall sign rule. This fact

provides strong support for previous arguments for the absence of topological order in systems satisfying the Marshall sign rule. Although these outcomes are in good agreement with recent DMRG calculations of Ref. 4, the gapless Dirac-type fermionic RVB ansatz remains slightly more accurate at the variational level in the highly frustrated regime.

ACKNOWLEDGMENTS

T.L. acknowledges financial support by the European Research Council under Research Grant SUPERBAD (Grant Agreement No. 240524). This work is also supported by NSFC Grant No. 10774187 and National Basic Research Program of China Grants No. 2007CB925001 and No.2010CB923004.

APPENDIX A: THE VARIOUS PHASES DESCRIBED BY THE WAVE FUNCTION STUDIED IN THIS WORK

The various phases described by the wave function studied in this work are shown in Fig. 6. Here, we report the various properties as functions of two parameters, namely, F/λ and Δ/λ . The case with nonzero F_{2x}/λ is qualitatively similar. The condensation lines denote the magnetically ordered states with staggered or collinear patterns. The three regions *A*, *B*, and *C* denote spin-liquid phases. In regions *A* and *B*, the spinon gap minimum is realized at the Γ point, while in the region *C* the gap minimum is moved to the *M* point. In region *B*, the Marshall sign rule is violated while it is satisfied in region *A*. The region with slanted lines is physically nonaccessible.

APPENDIX B: THE MEAN-FIELD FINITE-SIZE GAP

In the mean-field theory, the spinon is always gapped when the system is defined on a finite lattice. We report in Fig. 7 the spinon gap obtained by solving the mean-field self-consistent equations. Here, we would like to emphasize that the origin of a spinon gap obtained on finite lattices with the projected bosonic RVB wave function is totally different from that obtained within the mean-field approximation. Indeed, after projection, the number of spinons is fixed (each site is occupied by one and only one spinon) and the RVB wave function is always well defined.

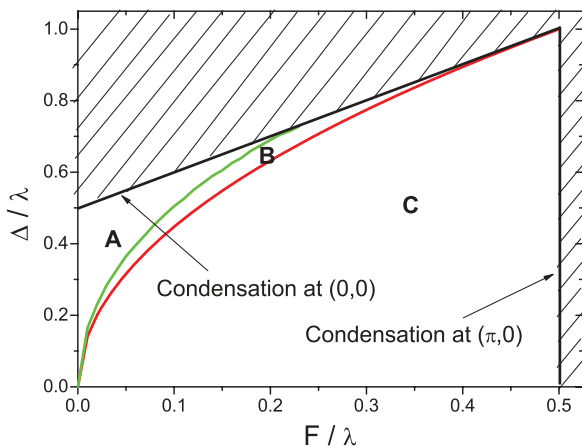


FIG. 6. (Color online) Phases described by the bosonic RVB wave function |RVB) in the parameter space $(F/\lambda, \Delta/\lambda)$.

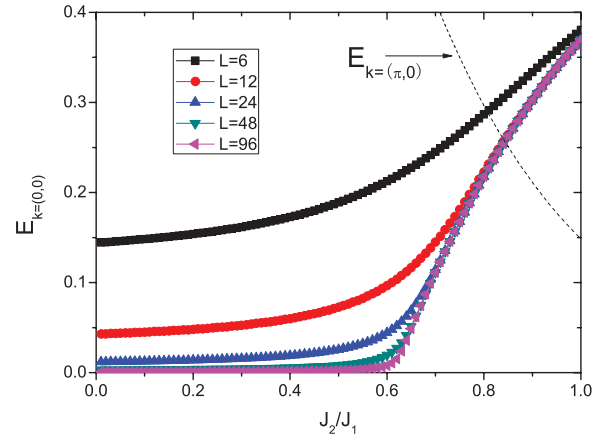


FIG. 7. (Color online) The spinon gap predicted by mean-field theory at both Γ and *M* points. For the Γ point, we show the scaling of the mean-field gap with the linear size of the system. The mean-field gap at the *M* point in the thermodynamic limit is also reported (dashed line).

In fact, we find that the spinon gap is exactly zero for $J_2 < 0.4J_1$ from our optimization on the 6×6 lattice; see Fig. 3. Instead, the finite-size gap in the mean-field theory is much larger and smoother than that obtained with the projected bosonic RVB wave function. In addition, we note that the mean-field theory always predicts a very large gap at the *M* point in the thermodynamic limit.

APPENDIX C: THE PROOF OF $\Delta_{k=(\pi,0)} = 0$

For the ansatz of type *A*, which is manifestly translationally invariant in the so-called uniform gauge, the gauge transformations of the PSG for symmetric bosonic spin-liquid state are found to be (we have adopted the convention of Ref. 29)

$$\begin{aligned} G_{P_x} &= \eta_{xP_x}^{i_x} \eta_{yP_x}^{i_y} e^{i\phi_x}, \\ G_{P_y} &= \eta_{yP_x}^{i_x} \eta_{xP_x}^{i_y} e^{i\phi_x}, \\ G_{P_{xy}} &= e^{i\phi_{xy}}, \end{aligned}$$

in which $\eta_{xP_x}, \eta_{yP_x} = \pm 1$, $\phi_x, \phi_{xy} = 0, \pi/2$.

If we require $\Delta_{i,j}$ to be nonzero between nearest-neighbor sites, the PSG should satisfy

$$\eta_{xP_x} = -\eta_{yP_x}, \quad \eta_{xP_x} = -e^{2i\phi_x}.$$

In the uniform gauge, $\Delta_{i,j}$ is a function only of $R_j - R_i$, so we can write $\Delta_{i,j}$ as $\Delta_{(d_x, d_y)}$, in which the distance $(d_x, d_y) = (j_x - i_x, j_y - i_y)$. By applying P_x and P_y successively, we have

$$\begin{aligned} \Delta_{(-d_x, -d_y)} &= (\eta_{xP_x} \eta_{yP_x})^{d_x+d_y} \Delta_{(d_x, d_y)} \\ &= (-1)^{d_x+d_y} \Delta_{(d_x, d_y)}. \end{aligned}$$

However, from the fact that $\Delta_{i,j} = -\Delta_{j,i}$, we have

$$\Delta_{(-d_x, -d_y)} = -\Delta_{(d_x, d_y)}.$$

We thus conclude that $\Delta_{i,j}$ is nonzero only between sites in the opposite sublattices.

To show further that $\Delta_{k=(\pi,0)} = 0$, we need to go to the sublattice uniform gauge.³² For $\phi_{xy} = 0$, the gauge transformation from the uniform gauge to the sublattice uniform gauge

is given by

$$W_i = (-1)^{[(i_x+i_y)/2]},$$

while for $\phi_{xy} = \pi/2$, it is given by

$$W_i = (-1)^{[(i_x-i_y)/2]},$$

in which $[r]$ means the largest integer that is not greater than r . In the sublattice uniform gauge, the pairing term $\Delta_{(d_x,d_y)}$ has s -wave symmetry from any site in the A

or B sub-lattice (but has opposite signs for $\Delta_{i,j}$ starting from the A and B sublattices). Thus the total contribution to the Fourier transform of $\Delta_{(d_x,d_y)}$ from distance (d_x,d_y) and all the other symmetry-related distances is proportional to

$$\Delta_{(d_x,d_y)}[\cos(k_x d_x) \cos(k_y d_y) + \cos(k_x d_y) \cos(k_y d_x)].$$

Since $\Delta_{(d_x,d_y)}$ is nonzero only when $d_x + d_y$ is an odd integer, it is easy to see that $\Delta_{k=(\pi,0)} = 0$.

-
- ¹P. W. Anderson, *Mater. Res. Bull.* **8**, 153 (1973).
²Z. Y. Meng, T. C. Lang, S. Wessel, F. F. Assaad, and A. Muramatsu, *Nature (London)* **464**, 847 (2010).
³S. Yan, D. A. Huse, and S. R. White, *Science* **332**, 1173 (2011).
⁴H.-C. Jiang, H. Yao, and L. Balents, *Phys. Rev. B* **86**, 024424 (2012).
⁵M. B. Hastings, *Phys. Rev. B* **69**, 104431 (2004).
⁶L. Capriotti, F. Becca, A. Parola, and S. Sorella, *Phys. Rev. Lett.* **87**, 097201 (2001); J. Richter and J. Schulenburg, *Eur. Phys. J. B* **73**, 117 (2010).
⁷S. Yunoki and S. Sorella, *Phys. Rev. B* **74**, 014408 (2006); D. Heidarian, S. Sorella, and F. Becca, *ibid.* **80**, 012404 (2009).
⁸Y. Ran, M. Hermele, P. A. Lee, and X.-G. Wen, *Phys. Rev. Lett.* **98**, 117205 (2007); M. B. Hastings, *Phys. Rev. B* **63**, 014413 (2000); Y. Iqbal, F. Becca, and D. Poilblanc, *ibid.* **84**, 020407(R) (2011).
⁹Tao Li, [arXiv:1101.1352](https://arxiv.org/abs/1101.1352).
¹⁰J. Schulz, T. A. Ziman, and D. Poilblanc, *J. Phys. I* **6**, 675 (1996).
¹¹N. Read and S. Sachdev, *Phys. Rev. Lett.* **62**, 1694 (1989).
¹²M. P. Gelfand, R. R. P. Singh, and D. A. Huse, *Phys. Rev. B* **40**, 10801 (1989).
¹³O. P. Sushkov, J. Oitmaa, and Z. Weihong, *Phys. Rev. B* **63**, 104420 (2001).
¹⁴M. Mambrini, A. Lauchli, D. Poilblanc, and F. Mila, *Phys. Rev. B* **74**, 144422 (2006).
¹⁵R. Darradi, O. Derzhko, R. Zinke, J. Schulenburg, S. E. Kruger, and J. Richter, *Phys. Rev. B* **78**, 214415 (2008).
¹⁶L. Wang, Z.-C. Gu, F. Verstraete, and X.-G. Wen, [arXiv:1112.3331](https://arxiv.org/abs/1112.3331).
¹⁷N. Read and S. Sachdev, *Phys. Rev. Lett.* **66**, 1773 (1991).
¹⁸P. Chandra and B. Doucot, *Phys. Rev. B* **38**, 9335 (1988).
¹⁹V. N. Kotov, J. Oitmaa, O. P. Sushkov, and Zheng Weihong, *Phys. Rev. B* **60**, 14613 (1999).
²⁰L. Capriotti and S. Sorella, *Phys. Rev. Lett.* **84**, 3173 (2000).
²¹S. Liang, B. Doucot, and P. W. Anderson, *Phys. Rev. Lett.* **61**, 365 (1988).
²²J. Lou and A. W. Sandvik, *Phys. Rev. B* **76**, 104432 (2007).
²³K. S. D. Beach, *Phys. Rev. B* **79**, 224431 (2009).
²⁴Y. C. Chen and K. Xiu, *Phys. Lett. A* **181**, 373 (1993).
²⁵Haijun Liao and Tao Li, *J. Phys.: Condens. Matter* **23**, 475602 (2011).
²⁶I. M. Wanless, in *Handbook of Linear Algebra*, edited by L. Hogben (Chapman and Hall/CRC, London/Boca Raton, FL, 2007), Chap. 31.
²⁷T. Tay and O. I. Motrunich, *Phys. Rev. B* **84**, 020404(R) (2011).
²⁸D. P. Arovas and A. Auerbach, *Phys. Rev. B* **38**, 316 (1988).
²⁹X.-G. Wen, *Phys. Rev. B* **65**, 165113 (2002).
³⁰F. Wang and A. Vishwanath, *Phys. Rev. B* **74**, 174423 (2006).
³¹L. Messio, C. Lhuillier, and G. Misguich, *Phys. Rev. B* **83**, 184401 (2011).
³²Here, we have adopted the sublattice uniform gauge rather than the uniform gauge. The mean-field ansatz in the sublattice uniform gauge is translationally invariant with a doubled unit cell. The gauge transformation relating the uniform gauge and the sublattice uniform gauge is given by $(-1)^{[(i_x \pm i_y)/2]}$ depending on the type of PSG; $[r]$ means the largest integer that is not greater than r .
³³F. Mila, D. Poilblanc, and C. Bruder, *Phys. Rev. B* **43**, 7891 (1991).
³⁴Given the fact that the computational cost for dealing with permanents grows exponentially with the number of lattice sites, an optimization procedure on the 8×8 cluster is not affordable. Moreover, an accurate estimation of the gap would require an accuracy on the energy that is not presently reachable.
³⁵As a result of the two-sublattice structure of the mean-field ansatz, $k = (0,0)$ is equivalent to $k = (\pi,\pi)$.
³⁶V. Lante and A. Parola, *Phys. Rev. B* **73**, 094427 (2006).
³⁷F. Becca, L. Capriotti, A. Parola, and S. Sorella, in *Quantum Spin Systems in Introduction to Frustrated Magnetism: Materials, Experiments, Theory*, edited by C. Lacroix, P. Mendels, and F. Mila, Springer Series in Solid-State Sciences Vol. 164 (Springer, Berlin, 2011), p. 379.
³⁸W. Marshall, *Proc. R. Soc. London, Ser. A* **232**, 48 (1955).
³⁹Tao Li and Hong-Yu Yang, *Phys. Rev. B* **75**, 172502 (2007); Tao Li, *Europhys. Lett.* **93**, 37007 (2011).